Nickel Electroplating On Steel From Acidic Citrate Baths

By M.A.M. Ibrahim, S.S. Abd El Rehim, S. M. Abd El Wahaab & M.M. Dankeria

Electroplating of nickel onto steel substrates from citrate baths has been investigated under different conditions of bath composition, current density, pH and temperature. A detailed study has been made of the influence of these variables on the potentiodynamic cathodic polarization curves, cathodic current efficiency and throwing power, as well as the throwing index of these baths. The optimum conditions for producing sound and satisfactory nickel deposits are: $NiSO_4 \cdot 6H_2O$ 100 g/L, trisodium citrate 25 g/L and citric acid 20 g/L at pH 5.0, with $i = 2$ A/dm^2 and at 25 °C. Moreover, the effect of sinusoidal a.c. superimposed on d.c. on electroplating of nickel from the optimum citrate bath has been investigated. The surface morphology of the as-plated nickel was investigated by using scanning electron microscopy (SEM) while the structure was studied by using X-ray diffraction analysis and anodic stripping voltammetry (ASV) techniques.

Nickel electrodeposits have widespread uses, such as increasing the life of industrial, transport, and service apparatus, and to give them decorative and functionally suitable metal coatings.[1] Moreover, because of favorable mechanical properties, nickel electrodeposits are used for electroforming of printing plates, phonograph record stampers, foil, tubes, screens and many other articles.[2] The selection of an electroplating bath depends primarily on the required characteristics of the nickel plate. Electrodeposition of nickel has therefore been studied by various authors using different baths.[3-15] Also, nickel electroplates are extensively studied from Watts-type baths in the presence of different organic brighteners.[16-18] In this study, electrodeposition of nickel from slightly acidic citrate baths has been investigated under different operating conditions, such as bath composition, pH, plating current density, superimposed a.c. on d.c., temperature and plating time to find the optimum conditions for producing sound and satisfactory deposits.

Experimental Procedure

All the plating bath constituents were reagent grade, using doubly distilled water. The composition of the baths used for nickel electrodeposition is given in Table 1. For electrodeposition, a steel cathode and platinum sheet anode, each 2.5 x 3.0 cm and 2.5 cm in height, were used. The plating cell used was a rectangular Perspex trough (10 x 3.0 cm) provided with vertical grooves on each sidewall, to fix the electrodes. Before each run, the steel cathode was mechanically polished with different grade emery papers: 600, 800, 1000 and 1500, then washed with distilled water, rinsed with ethanol and weighed. Direct current was supplied by a d-c power supply. The cathodic current efficiencies (CCE) were determined with the help of a Cu-coulometer ($CCE = Wt_{exp}/Wt_{theo}$) where Wt_{exp} is the weight of the deposit obtained experimentally and Wt_{theo} is the theoretical weight of the deposit according to Faraday's law. Most of the experiments were carried out at 25 ±2 °C. Plating duration was 20 min. In some experiments, a sinusoidal alternating current was superimposed on the d.c. by direct connection to the cathode and the anode. To obtain separation of the external d-c and a-c circuits, an induction coil (2.5 H, 0.25 A) was introduced in the direct-current circuit and a capacitor of 100 F, 12 V, was joined to the a-c circuit.

The throwing power (TP) of the solution was measured using a Haring-Blum rectangular Perspex cell fitted with one anode between two parallel cathodes where the ratio of the far to the near distance was (5:1). The percentage throwing power was calculated from Field's formula[19]

$$TP\% = \frac{L - M}{L + M - 2} \times 100$$

where L is the current distribution ratio or linear ratio (5:1) and M is the metal distribution ratio of the near to far cathodes.

In some cases, the values of M were measured as a function of L over a wide range of linear ratios varying between 1:1 and 5:1. The throwing index (T.I.) of each bath was considered as the reciprocal of the slope of the M vs. L plot.[20]

Potentiodynamic cathodic polarization measurements were performed in the rectangular cell. A potentiostat/galvanostat, controlled by PC was used for the potentiodynamic and the stripping voltammetric measurements. All potentials were measured relative to a saturated calomel electrode (SCE). To avoid contamination, the reference electrode was connected to the working steel cathode via a bridge provided with a Luggin-Haber tip and filled with the solution under test. The tip was placed very close to the electrode surface. All potentials were measured and recorded vs. the saturated calomel electrode.

Potentiodynamic anodic stripping voltammetric curves were obtained in a conventional electrolytic cell containing a platinum sheet cathode (2.5 x 3 cm) as a working electrode, a saturated calomel reference electrode and a platinum wire as a counter electrode. Deposition of Ni from the plating bath was carried out on the platinum sheet cathode at a constant deposition potential of -900 mV (SCE) for different plating times (50-600 sec). At the end of each deposition time, stripping analysis was performed immediately in the same plating bath (*in situ*) by sweeping the potential to more anodic values at a potential sweep rate of 5 mV/sec.

The surface morphology of the nickel electrodeposit was examined using a scanning electron microscope). The structure of the nickel deposit from the selected bath on steel cathodes was examined by X-ray diffraction analysis, using a diffractometer (40 kV, 25 mA) with Ni filter and Cu Kα radiation.

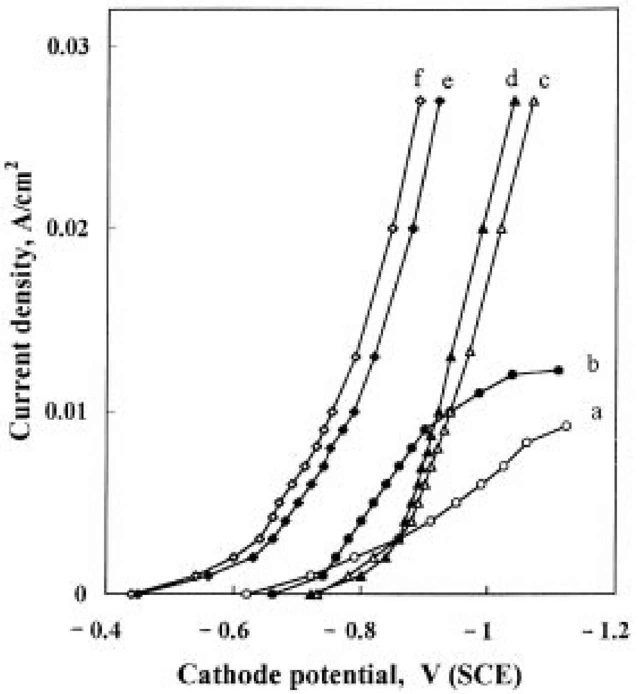

Fig. 1—Polarization curves during Ni-electrodeposition from different baths (Curve a, Bath No. 1; Curve b, No. 2; Curve c, No. 3; Curve d, No. 4; Curve e, No. 5; Curve f, No. 6).

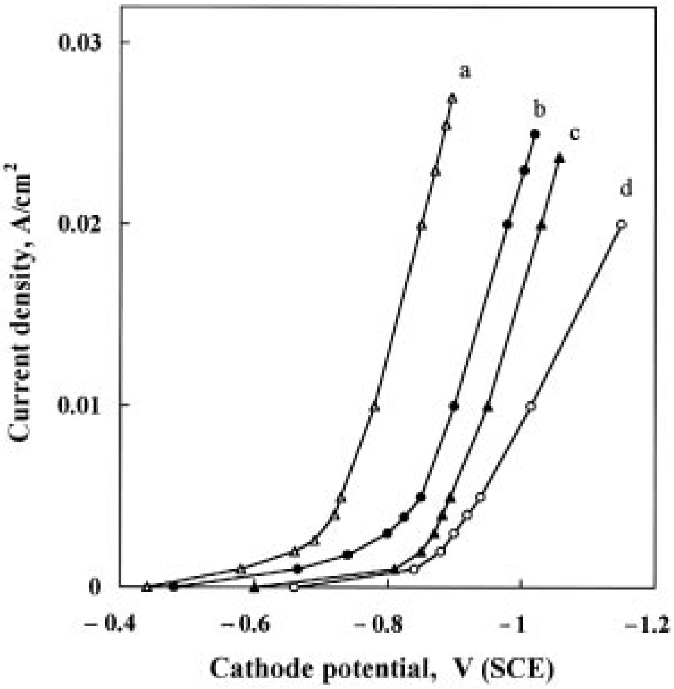

Fig. 2—Polarization curves during Ni-electrodeposition for different values of pH (Curve a, pH 3.1; Curve b, pH 4.0; Curve c, pH 5.0; Curve d, pH 6.0).

The microhardness of the nickel deposit was measured by a microhardness tester. In all tests, a 25 gf load was employed and the hardness (HV) was expressed in kgf/mm^2.

Results & Discussion

Cathodic polarization curves

The data of Fig. 1 represent the cathodic polarization curves for nickel deposition from Ni-1 to Ni-6 solutions (curves a-f). Inspection of the data reveals that the nickel deposition is accompanied by significant cathodic polarization. Also, the data show that in case of deposition from nickel sulfate solutions only, Ni-1 and Ni-2 solutions (curves a and b respectively), the current tends to attain a limited value that results, at least partially, from the deposition limitation by the diffusion of Ni^{+2} ions. Increasing the Ni^{+2} ion concentration in the electrolyte shifts the deposition potential of Ni to a less negative potential and enhances the limiting current value (curves a and b). Such behavior could be attributed to the decrease in the concentration (diffusion) overpotential.

Addition of trisodium citrate to the Ni-3 and Ni-4 solutions, however, changes the nature of the cathodic polarization curves (curves c and d) and these curves are characterized by an initial rapid potential shift to the more negative direction, followed by a gradual increase with rise of current density. Such a potential shift could be attributed to the formation of different soluble complex species. According to the literature[22,23] the following equilibrium constants K could be written as follows:

$$K(Ni^{+2} + H_2Cit^- = NiH_2Cit^+) \quad 0.56 \times 10^2 \qquad (1)$$
$$K(Ni^{+2} + HCit^{-2} = NiHCit) \quad 0.23 \times 10^4 \qquad (2)$$
$$K(Ni^{+2} + Cit^{-3} = NiCit^-) \quad 0.13 \times 10^6 \qquad (3)$$

From these equilibrium constants, we can conclude that the NiCit$^-$ is the predominant complex species in the solution because it has a much higher equilibrium constant. In addition, because the concentration of the total citrate ion is lower than the metal ion concentration, there will also be significant amounts of free Ni^{+2} present in the solution at all values of pH. The following electroreduction reactions are possible, therefore, with hydrogen evolution from independent side reactions:

$$Ni^{+2} + 2e^- = Ni \qquad (4)$$
$$NiCit^- + 2e = Ni + Cit^{-3} \qquad (5)$$

The inhibition effect of citrate ion (*i.e.*, the increase in cathodic polarization), especially at low current densities, could be assigned to the decrease in the concentration of the free Ni^{+2} as a result of complexation. In addition, citrate ions as such, or in the form of nickel complexes, may be adsorbed on the cathode surface and block the active sites available for the Ni discharge process.

In contrast, the presence of citric acid (Ni-5 and Ni-6 baths) shifts the cathodic polarization curves to less negative values (curves e and f). The change in cathodic polarization increases with increasing acid concentration. Such change in polarization could be ascribed to the decrease in the pH of the solution as a result of the addition of the acid (Table 1). It is suggested that a decrease in pH increases the concentration of the uncompleted Ni^{+2} ions in the bath. It is probable that decreasing the pH value of the bath allows decrease in the overpotential of the simultaneous hydrogen evolution reaction.

To clarify the influence of pH of the bath on cathodic polarization, a series of measurements was carried out, using solutions containing the same concentrations of nickel sulfate, tri-sodium citrate and citric acid, but of different pH values (pH 3.1-6.0). The pH value of each bath was adjusted by addition of NaOH solution. The results are shown in Fig. 2. It is clear that on increasing the pH value of the bath, the cathodic polarization increases.

The influence of temperature on the cathodic polarization (E-i curves) during nickel electroplating from the Ni-9 bath

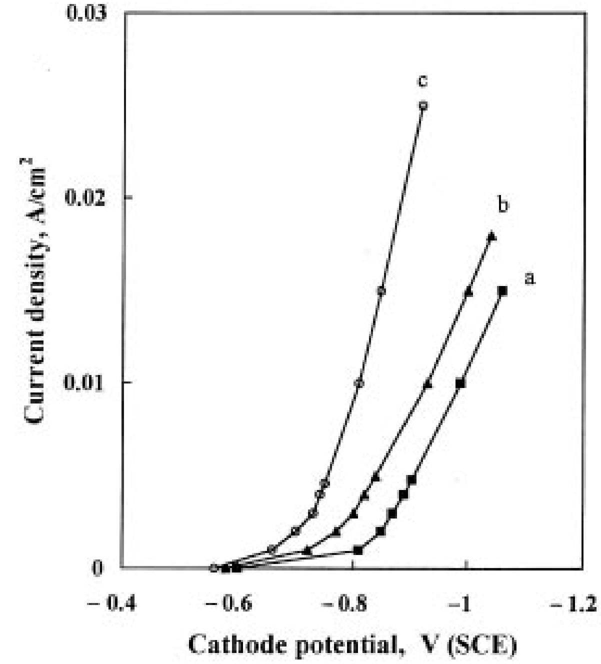

Fig. 3—Polarization curves during Ni-electrodeposition from Ni-9 bath at different temperatures (Curve a, 25 °C; Curve b, 35 °C; Curve c, 50 °C).

was examined and the results are shown in Fig. 3. The data reveal that a rise of bath temperature shifts the cathodic polarization curves to the less negative values. This behavior could be related to the decrease in the activation overpotential of both hydrogen evolution and nickel deposition reactions.[24] Moreover, an increase of temperature enhances the concentration of the reducible species in the diffusion layer as a result of increasing their diffusion rates. In addition to the effect of temperature on the relative abundance of both the completed and uncompleted species in the solutions, such behavior was obtained during the electrodeposition of cobalt from sulfate,[25] as well as from citrate[26] aqueous baths.

The cathodic polarization curves for nickel deposition from the Ni-9 bath were traced under the influence of sinusoidal superimposed a.c. Figure 4 shows that superimposed a.c. of a variable frequency, and a constant current density of 2 A/dm^2, shifts the cathodic polarization to the more negative values. This polarization-increasing effect of a.c. diminishes with increasing frequency. These data could be related to the fact that at low frequency, the time of a single oscillation is enough for rearrangement of the successive anodic and cathodic polarizations; thus the periodic fluctuation of the cathode potential is marked.

Table 1
Composition of Nickel Plating Solutions

Bath No.	Concentrations, g/L $NiSO_4 \cdot 6H_2O$	citric acid	tri-sod. citrate	C (Ω-cm)$^{-1}$	pH
Ni-1	60	—	—	15.2	6.8
Ni-2	100	—	—	21.1	6.8
Ni-3	100	—	10	23.4	6.2
Ni-4	100	—	25	25.9	5.9
Ni-5	100	10	—	24.0	2.4
Ni-6	100	20	—	25.2	2.3
Ni-7	100	20	25	25.5	3.1
Ni-8	100	20	25	30.7	4.0
Ni-9	100	20	25	32.2	5.0
Ni-10	100	20	25	32.5	6.0

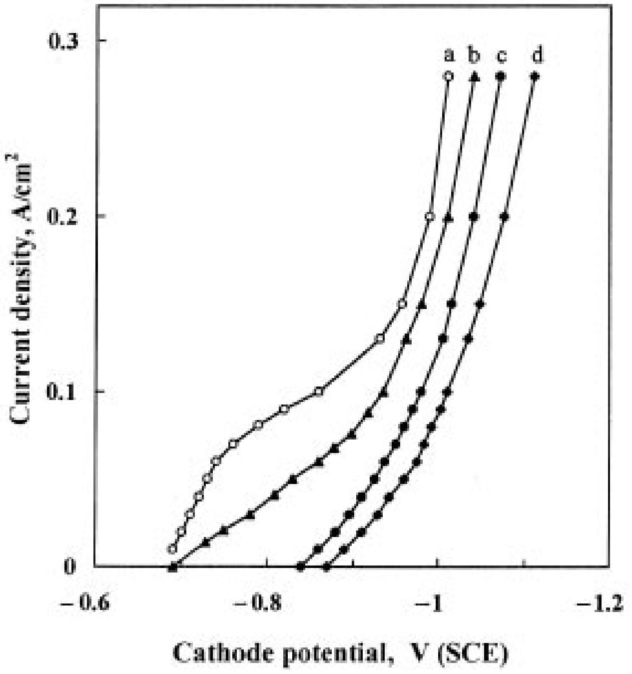

Fig. 4—Polarization curves during Ni-electrodeposition from Ni-9 bath with superimposed a.c. (i_{ac} = 2A/dm^2) of varying frequency (Curve a, 50 Hz; Curve b, 100 Hz; Curve c, 500 Hz; Curve d, 1000 Hz).

Cathodic Current Efficiency

The effect of both Ni content, as well as the citric/citrate ratio in the bath on the cathodic current efficiency, (CCE %), during nickel electrodeposition was studied as shown in Fig. 5. The data indicate that the CCE at a given pH (5.0) depends strongly on both the citric/citrate ratio and Ni content in the bath. At a given citric/citrate ratio, the CCE increases markedly with increase in nickel content in the bath, up to 120 g/L. Above this concentration, the CCE tends to level off at about 92 percent. At a given Ni content in the bath, the CCE is found to increase with increasing citric/citrate ratio.

The influence of pH on the cathodic current efficiency was studied in the pH range 3.1 to 6.0, using the bath of the optimum composition Ni-9 bath (Table 1); the data are listed in Table 2. It is clear that the efficiency of nickel deposition increases with increasing pH value of the bath from 3.1 to 5.0 and then levels off. This finding implies that the hydrogen evolution reaction was accelerated when the pH of the bath was relatively lower. These results agree well with the

Table 2
Effect of pH on Cathodic Current Efficiency, Throwing Power & Throwing Index for Ni-9 Bath

pH	CCE %	TP %	TI
3.1	16.4	19.2	1.4
4.5	85.3		
5.0	91.7	7.4	1.2
5.5	90.0		
6.0	90.0		

Time 20 min, 2 A/dm^2, 25 °C

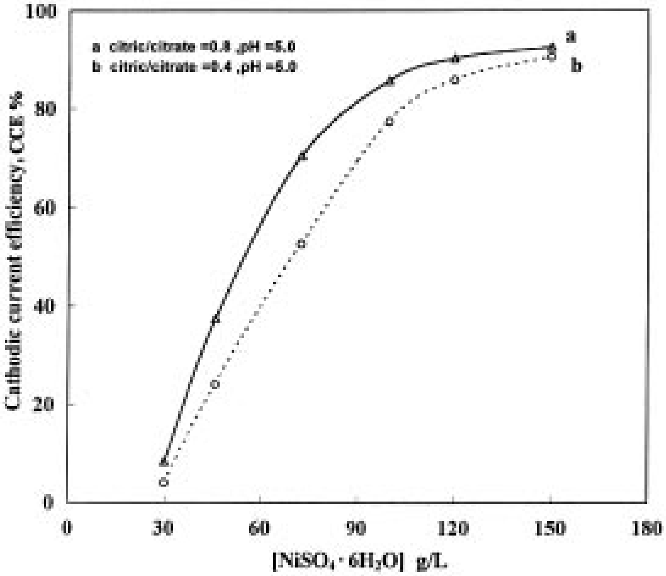

Fig. 5—The effect of [NiSO$_4$ · 6H$_2$O] concentration and the changed ratio of citric/citrate on the cathodic current efficiency at constant pH 5.0 (Curve a, citric/citrate ratio: 0.8; Curve b, Curve b, citric/citrate ratio: 0.4 (i = 2 A/dm^2, time = 20 min).

assumption that the shift in cathodic polarization curves towards the less negative direction with decreasing pH (Fig. 2) is related mainly to decrease in the overpotential of the hydrogen evolution reaction.

The influence of temperature on CCE for nickel deposition from the optimum bath Ni-9 at pH 5.0 is shown in Table 3. The data reveal that an increase of temperature from 25 to 70 °C has no significant effect on the CCE. This means that increasing bath temperature affects nearly equally both the deposition of nickel and the evolution of hydrogen. The remainder of the studies were carried out at a preferred room temperature of 25 °C.

The relation between the depositing current density and the cathodic current efficiency CCE from the Ni-9 bath is given in Table 4. The data reveal that the efficiency of Ni deposition decreases slightly with increasing current density. This finding suggests that a hydrogen evolution reaction will also take place as a side reaction on the cathode surface at a relatively high applied current density.

The influence of the duration of electrolysis was investigated using the optimum Ni-9 bath at i_{dc} = 2 A/dm^2 and at 25 °C. The results are included in Table 5. It is obvious that the cathodic current efficiency did not changed appreciably with duration time of electrolysis, indicating good bath stability.

Table 3
Effect of Temperature on Cathodic Current Efficiency, Throwing Power & Throwing Index for Ni-9 Bath

pH	CCE %	TP %	TI
25	91.7	7.4	1.2
35	84.2	29.2	1.8
50	84.9	38.2	2.2
60	89.3		
70	90.2		

Time 20 min, 2 A/dm^2, pH 5

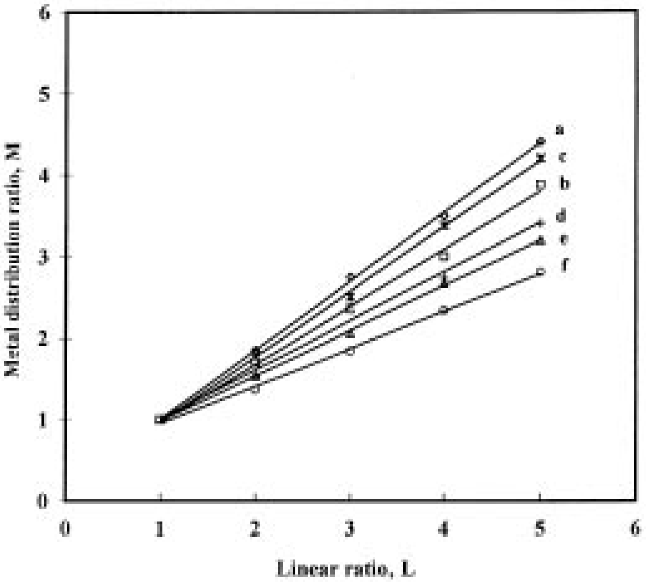

Fig. 6—Metal distribution ratio M vs. linear ratio L (NiSO$_4$ß6H$_2$O 100 g/L, trisodium citrate 25 g/L, citric acid 20 g/L); Curves: (a) i = 2 A/dm^2, pH 5.0, time 20 min, 25 °C; (b) i = 2 A/dm^2, pH 3.1, time 20 min, 25 °C; (c) i = 0.66 A/dm^2, pH 5.0, time 20 min, 25 °C; (d) i = 2 A/dm^2, pH 5.0, time 5 min., 25 °C; (e) i = 2 A/dm^2, pH 5.0, time 20 min, 35 °C; (f) i = 2 A/dm^2, pH 5.0, time 20 min, 50 °C.

From the above results, it is found that the optimum conditions for producing sound and satisfactory nickel deposits are: NiSO$_4$ · 6H$_2$O 100 g/L, trisodium citrate 25 g/L and citric acid 20 g/L (Ni-9 bath), at pH 5.0, i = 2 A/dm^2 and 25 °C.

A study has been conducted on the influence of superimposed a.c. of constant frequency and current density on the cathodic current efficiency of Ni deposition from the Ni-9 bath. The data are listed in Table 6. These data show that the superimposed a.c. on d.c. has no significant influence on the efficiency of Ni deposition. These results are in good agreement with the results obtained during the study of the effect of superimposed sinusoidal a.c. on nickel electroplating from acidic acetate solutions.

From the above mentioned data, it can be concluded that the cathodic current efficiency of nickel deposition from a citrate bath is slightly affected by the operating conditions, such as pH, current density, temperature, duration and the effect of a.c. superimposed on d.c.

Throwing Power and Throwing Index of The Bath

The throwing power (TP) of the Ni-9 bath was determined and the results show that its throwing power was poor and

Table 4
Effect of Current Density on Cathodic Current Efficiency, Throwing Power & Throwing Index for Ni-9 Bath

i A/dm^2	CCE %	TP %	TI
0.33	96.4		
0.66	96.9	11.1	1.3
1.00	91.3		
1.33	89.3		
1.66	92.3		
2.00	91.7	7.4	1.2

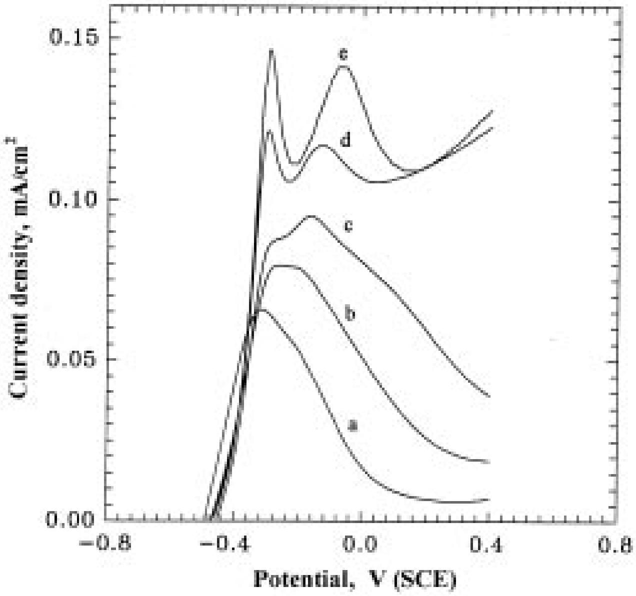

Fig. 7—Anodic stripping voltammograms of nickel deposit obtained from Ni-9 bath at deposition potential -900 mV and different deposition times (Curve a, 50 sec; Curve b, 100 sec; Curve c, 200 sec; Curve d, 300 sec; Curve e, 600 sec at scan rate of 5 mV/sec).

depended strongly on the operating conditions. Tables 2-5 include the values of TP under different conditions.

Lowering the pH of the Ni-9 bath gives rise to an increase in TP (Table 2), although it also gives rise to a depolarizing effect (Fig. 2). This could be explained by the slight increase in conductivity with increasing pH (Table 1). On the other hand, an increase in temperature of the Ni-9 bath improves the TP greatly, although it leads as well to the depolarizing effect (Fig. 3). This is expected from the fact that an increase in temperature increases the electrical conductivity of the bath. Moreover, increasing the applied current density or increasing the duration of deposition has a decreasing effect on the TP (Tables 4 and 5).

In general, the results of the throwing power study could be explained in terms of the two main factors that control this property. First, an increase of the cathodic polarization has an equalizing effect on the primary current distribution and so increased the throwing power.[27] Second, increase in the electrolytic conductivity results in improved throwing power. From these data, it is obvious that the role played by the electrical conductivity is greater than that played by the polarization effect.

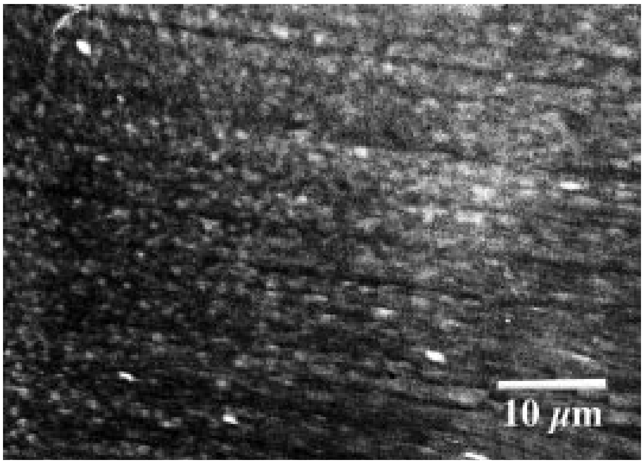

Fig. 8—Photomicrograph of nickel deposited from Ni-9 bath, 1500X, (time 20 min, i_{dc} = 2 A/dm^2, pH 5.0).

Another way of expressing the throwing power of the plating bath is the throwing index (TI). There are several advantages associated with expressing TP in the form of TI. For example, a single number is obtained, characteristic of a range of linear ratios. In addition, TI is obtained from several experimental points and thus minimizes errors in measurement of any one point.[20] The metal distribution ratio (M) is therefore plotted vs. the linear ratio (L), within the range from L = 1 to L = 5, as a function of various deposition conditions. Some representative results are shown in Fig. 6, which shows reasonable linear plots passing through the points represented by M = 1 and L = 1. The data of Tables 2-5 reveal that the calculated value of TI changes in a manner almost parallel to that observed for TP.

Table 5
Effect of Plating Time on Cathodic Current Efficiency, Throwing Power & Throwing Index for Ni-9 Bath

Time min	CCE %	TP %	TI
05	92.0	25.1	1.7
10	91.0		
15	91.3		
20	91.7	7.4	1.2
25	91.3		
30	92.0		

Surface Morphology & Structure of the Deposits

Black and rough nickel deposits were produced from baths containing nickel sulfate only (Ni-1 and Ni-2 baths). Addition of citrate ions into the bath, however, greatly improved the appearance and adherence of the deposits. Qualitative examination by simple procedures such as scrubbing, bending and heat/quench tests did not result in separation of the Ni deposit from the base metal, indicating good adherence. X-ray diffraction studies of the Ni deposits (as-deposited) showed two phases (α and β), each with face-centered-cubic (fcc) structure (Table 7).

A typical anodic stripping voltammogram (ASV) for Ni deposition from the optimum Ni-9 bath (pH 5, 25 °C) is shown in Fig. 7. The anodic scan exhibits two peaks corresponding to the two different phases. These results confirm the X-ray diffraction data.

Surface examination of as-plated nickel on steel substrate from citrate baths was carried out by scanning electron

Table 6
Effect of A-C Frequency & A-C Density On Cathodic Current Efficiency for Ni-9 Bath

Frequency Hz	CCE %	Current Density A/dm^2	CCE %
50	92.4	0.00	91.7
100	93.5	0.33	90.4
500	93.5	1.33	92.0
1000	93.5	2.00	92.4
		2.66	92.8

Time 20 min, 2 A/dm^2 ac/dc, pH 5, 25 °C, 50 Hz

Table 7
X-ray Diffraction Data of Nickel Deposited from Citrate Bath Ni-9

2θ	d, Å	I/I_0	hkl	Structure
44.58	2.0324	7.4	111	cubic
76.45	1.2460	100	220	α and β
92.94	1.0621	0.9	311	phases

Time 20 min, 2 A/dm^2, pH 5, 25 °C

microscopy (Fig. 8). The nickel deposited from the optimum bath Ni-9 at i_{dc} = 2 A/dm^2, 25 °C and t = 20 min. is compact, non-porous and composed of fine grains covering the entire surface. It is worthwhile to mention that most of the nickel deposited from the optimum bath under different operating conditions, such as current density, temperature and pH have more or less the same surface morphology as those in Fig. 8. The grains of nickel deposits from a citrate bath are more compact, with full coverage of the surface, than those obtained from different baths[7,28,29] which contain, under similar conditions, pitted dendritic grains, leaving some bare areas on the surface.

Microhardness of the Deposits

The microhardness of the nickel deposits from the citrate bath under different conditions was measured and the results are listed in Table 8. The data show that the microhardness of Ni is generally relatively high. It can be seen that microhardness of Ni deposits is influenced to some extent by bath composition as well as by the pH of the solution. The highest value of microhardness for nickel was produced from bath Ni-4, which contains nickel sulfate and trisodium citrate. Addition of citric acid (Ni-7 bath), however, decreased the hardness. This could be attributed to the fact that addition of citric acid lowers the pH of the solution and consequently enhances the hydrogen evolution reaction. The adsorbed hydrogen on the cathode surface may decrease the number of active sites of nucleation of nickel and therefore produce coarse-grain deposits characterized by low microhardness. This result could also be confirmed from the data given for Ni-9 (pH 5.0) and Ni-10 (pH 6.0) baths, as shown in Table 8, indicating that the microhardness increases with rise in pH of the bath.

Summary

Nickel deposits from acidic citrate baths can be produced using the following plating conditions: $NiSO_4 \cdot 6H_2O$ 100 g/L, trisodium citrate 25 g/L and citric acid 20 g/L at pH 5.0, i = 2 A/dm^2, t = 20 min at 25 °C. Under these conditions, the cathodic current efficiency is high (91.7%). The high CCE is found to be slightly affected by the operating conditions, such as pH, current density, duration and the effect of a.c. superimposed on d.c. The throwing power of these baths is poor (7.4%) and strongly dependent on the operating conditions. The surface morphology of the as-plated Ni deposit was examined by SEM, with the results revealing that the nickel deposits obtained from the optimum conditions are composed of compact, non-porous fine grains covering the entire surface. X-ray diffraction analysis (XRD) and anodic stripping voltammetry (ASV) proved that the Ni deposit under the optimum conditions consists of a mixture of two phases, α and β.

Table 8
Microhardness of Nickel Deposit under Conditions of Different Bath Constituents, pH & Current Density

Bath No.	HV kgf/mm^2
Ni-4	632
Ni-7	553
Ni-9	426
Ni-10	600

Time 60 min, 25 °C

Editor's note: *Manuscript received, June 1998; revision received, September 1998.*

References

1. G.G. Gawrilov, *Chemical (Electroless) Nickel-plating*, Portcullis Press Ltd., Redhill, Surrey, UK, 1979; p. 12.
2. F.A. Lowenheim, *Modern Electroplating*, Wiley Interscience, New York, NY, 1963; p. 286.
3. C.Q. Cui & J.Y. Lee, *Electrochim. Acta*, **40,** 1653 (1995).
4. W.G. Proud & C. Mueller, *Electrochim. Acta*, **38,** 405 (1993).
5. A.J. Dill, *Plating*, **61,** 1001 (Nov. 1974).
6. K. Kamel, *Materials Trans., JIM*, **30**, 251 (1989).
7. S.M. Abd El Wahaab, A.M. Abd El-Halim, S.S. Abd El Rehim & E.A. Abd El Meguid, *Surf. Technol.*, **29**, 313 (1986).
8. M. Fleishmann & A. Saraby-Reintjes, *Electrochim Acta*, **29**, 557 (1984).
9. P.V. Brande, A. Dumont & R. Winand, *J. Appl. Electrochem.*, **24,** 201 (1994).
10. E. Chassaing, M. Joussellin & R. Wiart, *J. Electroanal. Chem.*, **157,** 75 (1983).
11. Chr. Bozhkov & St. Rashkov, *Bull. Electrochem (India)* **5**, 756 (1989).
12. Chr. Bozhkov, Chr. Tzvetkova & St. Rashkov, *J. Electroanal. Chem.*, **296**, 453 (1990).
13. C. Kollia, N. Spyrellies, J. Amblard, M. Froment & G. Maurin, *J. Appl. Electrochem.*, **20**, 1025 (1990).
14. W. Dahms, R. Schumacher & J.M. McCaskie, *Plat. and Surf. Fin.*, **84,** 120 (May 1997).
15. C.B. Nielson, A. Horsewell & M.J. Ostergard, *J. Appl. Electrochem.*, **27,** 839 (1997).
16. C. Gao, Y. Lu & R. Liu, *Plat. and Surf. Fin.*, **84**, 83 (Sept. 1997).
17. H. Brown, *Trans. Inst. Met. Fin.*, **47**, 63 (1969).
18. T. Mimani, S.M. Mayanna & N. Munichandraich, *J. Appl. Electrochem.*, **239**, 339 (1993).
19. S. Field, *Metal Ind. (London)*, **44**, 416 (1934).
20. R.V. Jelinek & H.F. David, *J. Electrochem. Soc.*, **104**, 279 (1957).
21. L.G. Sillen & A.E. Martell *Stability Constants of Metal-Ion Complexes*, Chemical Soc., London, 1971; p. 413.
22. E. Hogefeldt & A.E. Martell *Stability Constants*, Special Publication No. 17, London, the Chemical Soc., Burlington House, W1 1964, p. 479.
23. A.Y. Ying & K.N. Patrick, *J. Electrochem. Soc.*, **135,** 2964 (1988).
24. V.B. Singh & P.K. Tikoo, *Electrochim. Acta*, **22**, 1201 (1977).

25. A.M. Abd El Halim, M.H. Fawazy & M.A. Mahmoud, *Trans. Inst. Met. Fin.*, **71**, 48 (1993).
26. S.S. Abd El Rehim, S.M. Abd El Wahaab, M.A.M. Ibrahim & M.M. Dankeria, *J. Chem. Tech. and Biotech.*, **JCTB**, 290 (1997).
27. E. Raub & K. Muller, *Fundamentals of Metal Deposition*, Elsevier, Amsterdam, 1967; p. 203.
28. C.Q. Cui & Jim Y. Lee, *Electrochim. Acta*, **40**, 1653 (1995).
29. M.H. Fawzy, M.M. Ashour & A.M. Abd El-Halim, *Trans. IMF*, **74**(2), 72 (1996).

About the Authors

Dr. Magdy A.M. Ibrahim is a lecturer of physical chemistry in the Chemistry Department, Ain Shams University, Abbassia, Cairo, Egypt. He holds MSc and PhD degrees in electrochemistry from Ain Shams University. He held a scholarship in Germany at Erlangen-Nuremberg University (1992-1994). He is an active member of the Egyptian Corrosion Society. His research interests are in electroplating of metals and alloys, corrosion of metals and the electrochemistry of some organic compounds.*

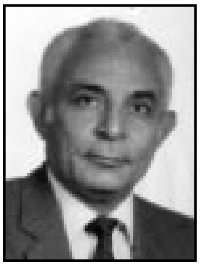

Dr. S.S. Abd El Rehim is professor of electrochemistry in the Chemistry Department, Ain Shams University, Cairo. He holds a PhD from the Hungarian Academy of Science. Prof. Abd El Rehim is an active member of the Egyptian Corrosion Society. He was awarded the State Prize for Encouragement in Chemistry in 1986 from the Egyptian Academy of Scientific Research and Technology. He has published more than 100 papers in international journals. His research interests are in electroplating of metals and alloys and corrosion of metals in aqueous media.

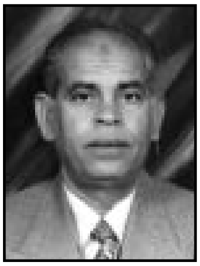

Dr. S.M. Abdel Wahaab is professor of electrochemistry in the Chemistry Department, Ain Shams University, Cairo. He holds a PhD from Moscow University. He is an active member of the Egyptian Corrosion Society. His research interests are in electroplating of metals and alloys, and corrosion of metals in aqueous media.

Marwan M. Dankeria is a doctoral candidate at Ain Shams University. He holds an MSc in the field of electrochemistry from Ain Shams University.

** To whom correspondence should be addressed.*